Time-Resolved Raman Spectroscopy with Subpicosecond Resolution: Vibrational Cooling and Delocalization of Strain Energy in Photodissociated (Carbonmonoxy)hemoglobin†

J. W. Petrich,‡ J. L. Martin,*,‡ D. Houde,‡ C. Poyart,§ and A. Orszag‡

Laboratoire d'Optique Appliquée, Ecole Polytechnique, ENSTA, INSERM U275, 91128 Palaiseau Cedex, France, and INSERM U299, 94275 Le Kremlin-Bicêtre, France

Received March 19, 1987; Revised Manuscript Received June 2, 1987

ABSTRACT: A Raman spectrometer that provides both subpicosecond resolution and independent, tunable pump and probe pulses is described. The spectrometer is employed to obtain time-resolved spectra of (carbonmonoxy)hemoglobin (HbCO) at times from 0.2 to 95 ps subsequent to ligand photodissociation. The spectra are interpreted in terms of a vibrationally hot heme that cools substantially in 10 ps. Concomitant with the proposed vibrational cooling is a slower relaxation, which we suggest results from a protein response to heme doming induced by ligand detachment. Results and interpretations are discussed in the context of current models of the heme photophysics and of hemoglobin reactivity.

Hemoglobin (Hb) is a tetrameric protein in equilibrium between two alternative quaternary structures: the unligated, low oxygen affinity, T ("tense") structure and the ligated, high oxygen affinity, R ("relaxed") structure. A study of the coupling between the heme and the protein during the transmission of this "heme–heme interaction" is essential for an understanding of the transition from the R to the T state.

The free energy difference between the R and T structures is ~3.6 kcal/mol of heme (Perutz, 1976). This stored energy is commonly referred to as the strain energy of cooperativity. Neither the degree of delocalization of this energy nor the time scale on which it is used by the protein is yet known. It is believed that the free energy of cooperativity lies both in weak bonds within the subunits of the tetramer and in changes in intersubunit constraints such as the rupture or formation of salt bridges. The amount of cooperative energy localized transiently at a heme site is, however, still to be evaluated.

One approach in the investigation of the heme–heme interaction is to identify the structures formed subsequent to ligand detachment. Both transient absorption and Raman spectroscopies have been used extensively to monitor the relaxation of the heme and the surrounding protein after dissociation of the bound ligand. These techniques have produced several pieces of evidence suggesting that, subsequent to ligand photodissociation, the heme and specific portions of its immediate protein environment attain a configuration similar to that of the equilibrium unligated heme. Findsen et al. (1985a) have shown that at 25 ps the Fe–histidine stretching frequency at 230 cm^{-1} (a marker of unligated, domed hemes) in adult human HbCO photoproduct is the same as that at 10 ns. Transient absorption measurements (Martin et al., 1983, 1984a; Petrich et al., 1987) indicate that a "deoxy-like" species occurs for all ligated heme proteins with a time constant of 300–350 fs. Until now, time-resolved absorption spectroscopy has been the only technique available for observing kinetics on a femtosecond time scale. Absorption spectroscopy is not likely, however, to be very sensitive to structural changes of the heme or to the influence of the environment on the heme. Thus, time-resolved resonance Raman spectroscopy has been exploited as a more sensitive method of obtaining detailed structural information concerning the dynamics of protein–heme interactions (Friedman et al, 1982a); however, until now, resonance Raman spectra of heme proteins have not been obtained with time resolution better than 25–30 ps (Findsen et al., 1985a,b; Campbell & Friedman, 1986; Terner et al., 1981; Dasgupta et al., 1985). We note that various theoretical methods have been used to relate absorption spectra and Raman excitation profiles and to identify the sources of spectral line broadening in biological molecules [see, for example, Schomaker and Champion (1986) and Myers et al. (1982)].

In order to investigate the structural changes involving the heme and the immediate protein matrix on the time scale of the formation of the deoxy-like product, we have constructed a Raman spectrometer capable of subpicosecond resolution. The spectrometer provides both a tunable pump beam, which can be used for the photodissociation of heme proteins, and a tunable probe beam of 30-cm^{-1} bandwidth. Here we present a description of the Raman spectrometer and a series of resonance Raman spectra of the ν_4 mode of HbCO taken from 0.2 to 95 ps subsequent to ligand photodissociation.

Experiments (Kitagawa et al., 1978) and normal coordinate analyses (Abe et al., 1978) have attributed ν_4 to the polarization-dependent, totally symmetric (A_{1g}) stretching mode of the $C_\alpha N$ bond of the heme. More specifically, this mode is assigned to a pyrrole ring breathing-like motion that is deformed by a large contribution from the $C_\alpha N$ stretching vibration. In ν_4, the four pyrrole rings vibrate in phase and the four nitrogen atoms are displaced toward the central metal ion (Abe et al., 1978; Kitagawa et al., 1976, 1977). Steady-state resonance Raman studies of heme proteins and model compounds have shown that ν_4 (1) is approximately 1355 cm^{-1} in deligated hemes and in the 1370s for ligated ferrous hemes (Yamamoto et al., 1973; Spiro & Burke, 1976; Rousseau et al., 1984) [at 1357 cm^{-1} in Hb and at 1373 cm^{-1} in HbCO (Friedman et al., 1982a; Asher, 1981)], (2) is sensitive to electron-withdrawing formyl groups substituted at the heme periphery (Tsubaki et al., 1980), and (3) shifts to higher frequencies upon oxidation of Fe(II) to Fe(III) (Rousseau et

† J.W.P. is the recipient of an NSF Industrialized Countries postdoctoral fellowship and an INSERM poste orange. D.H. was an NSERC postdoctoral fellow. Parts of this work were funded by INSERM, ENSTA, and Le Ministère de la Recherche et de la Technologie.

* Author to whom correspondence should be addressed.

‡ INSERM U275.

§ INSERM U299.

0006-2960/87/0426-7914$01.50/0 © 1987 American Chemical Society

al., 1984; Choi et al., 1982) or when the Fe is substituted with Ni(II) (Kitagawa et al., 1978; Choi et al., 1982). It is thus believed that factors which produce an increase in the π electron density of the porphyrin ring, and hence an increase in the electron density of the π^* antibonding orbitals of the porphyrin ring, will weaken the $C_\alpha N$ bond and decrease the ν_4 stretching frequency. Factors that can increase the π electron density of the porphyrin ring are disruption of back-bonding of iron $d\pi$ electrons to π acceptor ligands (e.g., O_2 and, to a lesser extent, CO) (Spiro & Burke, 1976) or a reduced nuclear charge of the metal [Fe(II) vs Ni(II) and Fe(III)] (Choi et al, 1982). Thus, the position of ν_4 has been used as a probe of the π electron density of the porphyrin ring and, consequently, as a probe of the extent of dissociation of ligated heme complexes (Friedman et al., 1982a; Asher, 1981). Spiro and co-workers have demonstrated that ν_4 is insensitive to the porphyrin core size and have suggested that heme doming has little affect on its value (Choi et al., 1982).

Our time-resolved spectra of the ν_4 mode of the HbCO photoproduct reveal a large initial downshift of the ν_4 mode of the HbCO photoproduct with respect to that of equilibrium unligated Hb. This downshift attains a minimum within 10 ps subsequent to photodissociation. The decay of the downshift is accompanied by a slower increase that becomes apparent 30 ps subsequent to photodissociation. The biphasic response of the ν_4 mode is discussed in terms of current models of the heme photophysics and of hemoglobin reactivity.

Experimental Procedures

(*A*) *Laser System.* Preliminary reports of our subpicosecond resonance Raman spectrometer have been given elsewhere (Petrich et al., 1987; Houde et al., 1986). Since those initial reports significant improvements have been made, leading to a much better signal-to-noise ratio. Here we give a more detailed description of our apparatus.

Pulses of approximately 60-fs duration are obtained from an eight-mirror, colliding-pulse ring laser with four intracavity prisms to compensate for dispersion. These pulses are amplified to ~1 mJ at 10 Hz with the second harmonic of a Nd:YAG (yttrium aluminum garnet) laser (Quantel). Thorough descriptions of the generation and amplification of short pulses have been given previously (Martin et al., 1982, 1983, 1984a, 1986; Fork et al., 1983). For our resonance Raman investigation of the ν_4 mode of the HbCO photoproduct, we use a photodissociative pump beam at 575 nm and a probe beam providing Soret enhancement at 435 nm (the absorption maximum of unligated Hb). To obtain the pump and probe beams, we further exploit the technique of continuum amplification (Martin et al., 1982, 1983, 1984a, 1986). The train of 1-mJ, 100-fs pulses from the four-stage amplifier is split into two beams and used to generate two continuua in 5-cm cells containing water. The 575-nm photodissociative pulse is obtained directly by selecting a 50-Å bandwidth from one continuum with an interference filter and amplifying it in a cell of rhodamine 6G in H_2O that is 2% Ammonyx LO (lauryldimethylamine oxide) (Franconyx, France) pumped with approximately 200 mJ of the YAG second harmonic. The resulting pump pulse has a duration of 120 fs and an energy of 0.8–1.0 mJ. The ratio of pulse energy to amplified spontaneous emission (ASE) is $\geq$20:1.

Attaining, however, a probe pulse that can provide both the necessary spectral resolution (approximately 30 cm^{-1}) and still afford subpicosecond temporal resolution demands additional attention. The requirement for a probe bandwidth not greater than 30 cm^{-1} (approximately 6 Å at 435 nm) prevents us from directly selecting from the continuum a 6-Å bandwidth centered at 435 nm and amplifying it. This limitation is due to the fact that such a small portion of the continuum contains very little energy (on the order of 0.5 μJ). While in principle such low energies can easily be amplified to the millijoule level, such a gain requires several stages of amplification. Essential to the operation of an amplifier chain is the presence of saturable absorbers between stages to discriminate the femtosecond laser pulse from the attendant ASE. When the gain medium in the amplifier is a rhodamine dye, an easily available, efficient saturable absorber can be found in malachite green. There is not, unfortunately, any saturable absorber equivalent to malachite green for a gain medium in the blue region of the spectrum, and thus the option of direct amplification of a 6-Å bandwidth at 435 nm is precluded.

To circumvent this problem, we select from the second continuum a narrow bandwidth centered at 870 nm and amplify this with two stages of LDS 867/MeOH, each pumped with 80 mJ of the YAG second harmonic. The amplified pulse at 870 nm (200 μJ) is frequency-doubled in a KDP or $LiIO_3$ crystal of 5-mm thickness. The nonlinear crystal serves the 2-fold function of producing the desired probe wavelength and removing the ASE generated by the infrared amplifiers. The 435-nm pulse (10 μJ) is then amplified in a coumarin 440/MeOH cell pumped with 120 mJ of the YAG third harmonic. The ASE from the coumarin cell is removed by spatial filtering and with an interference filter of 6-Å bandwidth centered at 435 nm (Barr Associates). The energy of the probe pulse, measured after the filter, is 80 μJ. The probe pulse is transform-limited with a duration of approximately 500 fs. The ratio of pulse energy to ASE is approximately 10:1. A diagram of the experimental apparatus is given in Figure 1.

(*B*) *Preparation and Handling of the Sample.* Solutions of pure hemoglobin A (HbA) were prepared from human adult red cell hemolysates by diethylaminoethyl-Sephadex column chromatography and a linear pH gradient from pH 7.9 to 6.9 in 50 mM 2-[bis(2-hydroxyethyl)amino]-2-(hydroxymethyl)-1,3-propanediol (bis-tris) hydrochloride buffer. The purity of the isolated HbA was verified by isoelectric focusing, which revealed a single band migrating at pH 6.95. HbA was freed of remaining small anions by passing the solution through a mixed-bed ion-exchange resin (Bio-Rad AG501-X8), concentrated under gas pressure in a Diaflo Amicon cell, and kept frozen in small droplets in liquid nitrogen until used. Our samples contained less than 1% methemoglobin.

Stock solutions of pure HbA were diluted to 0.5 mM (heme) in 0.1 M NaCl and 50 mM bis-tris HCl buffer at pH 7.0. The Hb solutions were completely deoxygenated at 25 °C in a glass tonometer under humidified pure argon. HbCO solutions were prepared by equilibrating Hb with pure CO.

The sample is placed in a small sealed cuvette and is translated through the pump and the probe beams at a velocity of 12 mm/s. This method induces no detectable sample damage: the same sample can be used over the period of 1 or 2 days without any degradation of its steady-state absorption spectrum or of its Raman spectrum. Moreover, using a cuvette instead of a jet does not prohibit the study of samples that cannot be produced in large quantities or which are air sensitive. Finally, the alignment and calibration is facilitated by interchanging the sample cell with an analogous cell containing a calibration standard such as CCl_4 or benzene.

(*C*) *Data Collection.* Zero time between the pump and the probe pulses is taken as the inflection point of the rise time of the photoinduced absorption at 435 nm of a sample of HbCO, which is determined in a parallel transient absorption experiment. The time resolution of our system (and the ab-

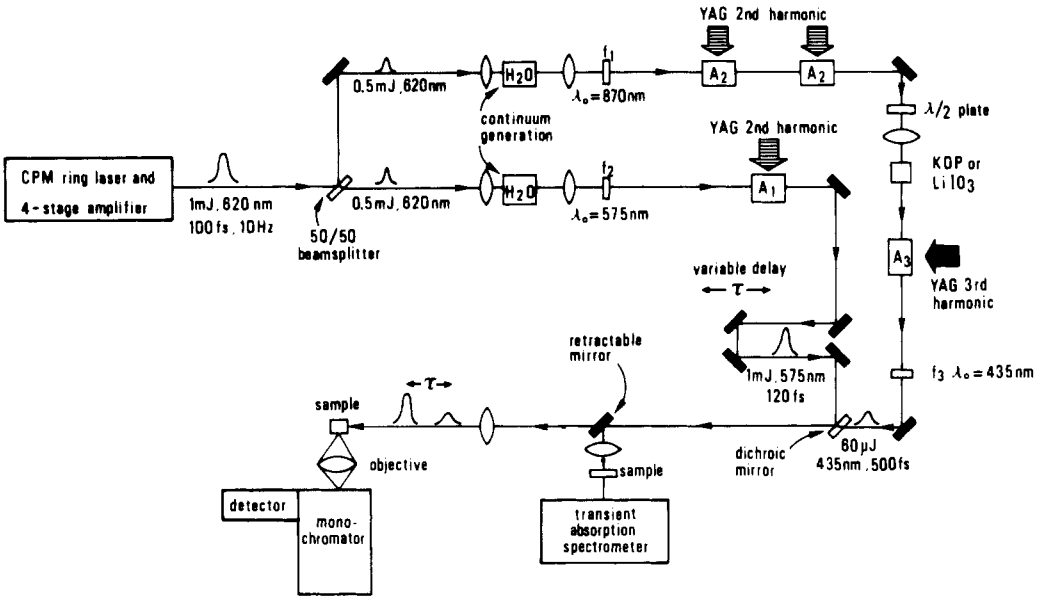

FIGURE 1: Apparatus for obtaining time-resolved Raman spectra. f_1 and f_2 are filters that are chosen to select portions of the continua for subsequent amplification. A_1, A_2, and A_3 are amplifier cells where the gain medium is rhodamine 6G, LDS 867, and coumarin 440, respectively. f_3 is an ~6-Å filter centered at 435 nm that discriminates the 500-fs probe pulse from ASE. Transient absorption spectra can be obtained by using the retractable mirror to direct the pump and the probe beams into the absorption spectrometer. See text for further details.

sence of jitter between pulses) is verified by monitoring the rise time of the absorption at 435 nm, which is the integral of the convolution of the pump pulse, the probe pulse, and the molecular response [the time constant for the appearance of the deoxy-like species, approximately 350 fs in HbCO (Martin et al., 1983, 1984a; Petrich et al., 1987)].

Transient Raman spectra are obtained by focusing the pump and the probe beams to approximately 300 μm in the sample at room temperature (15 °C). We attenuate the pump energy to ~500 μJ, which is below the threshold for photoinduced sample damage and continuum generation. Under these conditions, we dissociate 40 ± 5% of the HbCO. The extent of photodissociation is a quantity that is measured independently in a transient absorption experiment. The pump and the probe are polarized in the same direction, and their polarization vectors lie perpendicular to the line containing the collection optics and parallel to the plane of the optical table. No polarization analyzer or depolarizer is employed. An $f/0.95$ objective collects and focuses the Raman scattering into a single-stage $f/8$ monochromator with a 1200 L/mm grating blazed at 5000 Å (Jobin-Yvon). A slit width of 230 μm is used. Data are collected with a gated OMA III (EG&G Electronics) whose detector is cooled to −33 °C to maximize uninterrupted integration time. Each spectrum represents the sum of three spectra taken with a 12-min integration time from which a corresponding 12-min background spectrum was subtracted. The resultant spectrum is smoothed once and normalized with respect to a spectrum obtained with only the probe beam. This normalization takes into account the fluctuations in the probe beam and the fact that the Raman scattering is absorbed more strongly in a sample containing unligated Hb. Difference spectra are obtained by subtraction of the HbCO spectrum taken with the probe beam only. A flat difference spectrum is obtained by subtraction of the probe-only spectrum from the −5-ps spectrum. Spectra are reproducible to within 0.8 cm^{-1} (the frequency separation between adjacent pixels of our detector). That the amount of photodissociation induced by the probe beam itself is small is demonstrated by the position and the shape of the ν_4 band in HbCO as compared with its equilibrium unligated Hb counterpart (Figure 2).

As can be seen from Figure 2, the Raman bands of the equilibrium spectra are as narrow as allowed by the spectral bandwidth of our probe pulse. Specifically, the full width of half-maximum (fwhm) of the ν_4 band of the unligated equilibrium Hb (approximately 34 cm^{-1}) is what one would expect from the convolution of a 30-cm^{-1} Gaussian laser pulse and a 14.7-cm^{-1} Gaussian spectral line for the Hb (Friedman et al., 1982a,b).

(D) Data Analysis. A determination of the shift and of the broadening of the bands of the HbCO photoproduct with respect to their counterparts in unligated equilibrium Hb is central to the interpretation of our data. Had we been able to dissociate 100% of the HbCO, it would have been possible to extract directly the shift and the broadening of the ν_4 band of the HbCO photoproduct. Since the ν_4 bands of equilibrium Hb and HbCO are separated by "only" 16 cm^{-1} (Figure 2), the photoproduct spectra obtained with incomplete dissociation do not permit a direct determination of the shift or the broadening of the ν_4 band of the photoproduct. This prompted us to produce difference spectra of the HbCO photoproducts by subtraction of the equilibrium HbCO spectrum (Figures 3 and 4).

Rousseau and co-workers (Friedman et al., 1982a; Rousseau et al., 1984; Rousseau, 1981) have shown that difference spectra are especially sensitive to small shifts in band positions, and Laane and Kiefer (1980) have provided a detailed description of the effects of shifting, broadening, and the combination of shifting and broadening on difference spectra. The conclusions of these studies most relevant to this work are the following:

(1) Asymmetry in a difference spectrum can be a consequence *only* of a spectrally broadened photoproduct, and the shape of the difference spectrum is independent of the amount of photoproduct produced, *providing* the sum of the integrated area of the spectra of the photoproduct and the undissociated species is equal to the integrated area of the band obtained before photodissociation and the functional form of the undissociated species and the photoproduct is the same.

(2) Changes in the shape of a difference spectrum are easily noted by monitoring the frequency at which the difference spectrum equals zero, i.e., the position of the inflection point.

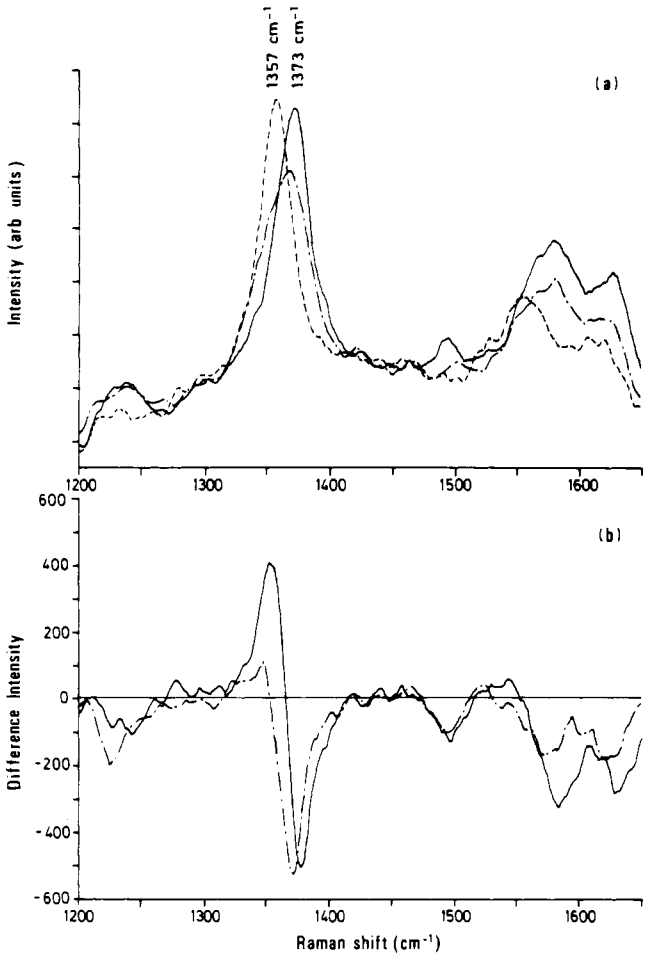

FIGURE 2: (a) High-frequency portion of the resonance Raman spectra of equilibrium HbCO (—), equilibrium Hb (– – –), and the HbCO photoproduct 0.2 ps subsequent to ligand dissociation (–·–) obtained with 435-nm, 500-fs, and 80-μJ probe pulses. The fwhm of the equilibrium spectra (approximately 34 cm^{-1}) is what one would predict from the convolution of a 30-cm^{-1} Gaussian pulse and a 14.7-cm^{-1} Gaussian spectral band. (b) Difference spectrum obtained by subtracting the HbCO spectrum from the Hb spectrum (—). Note the near symmetry of the difference spectrum of the ν_4 band in the region from 1350 to 1375 cm^{-1}. This symmetry reflects the fact that the only significant difference between ν_4 in the equilibrium HbCO and Hb species is a spectral shift. Also displayed is the difference spectrum obtained by subtracting the HbCO spectrum from the 0.2-ps photoproduct spectrum (–·–).

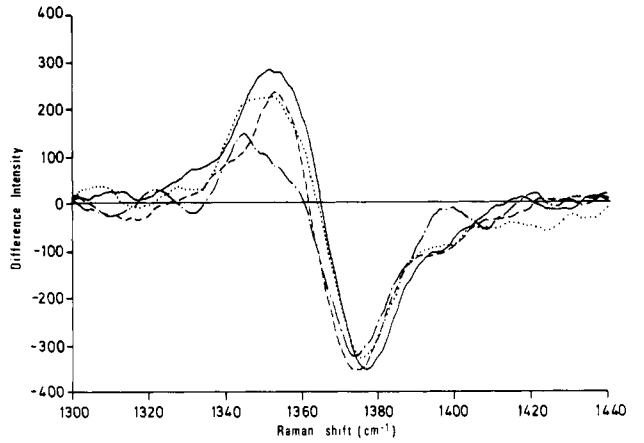

FIGURE 3: Resonance Raman difference spectra obtained by subtracting the equilibrium HbCO spectrum from various HbCO photoproduct spectra: 0.9 (–·–), 2 (– – –), 9.4 ps (···), and equilibrium unligated Hb (—). The decrease in the downshift of these spectra with respect to the equilibrium unligated Hb and the attendant increase in symmetry as a function of time is attributed to vibrational cooling of the heme.

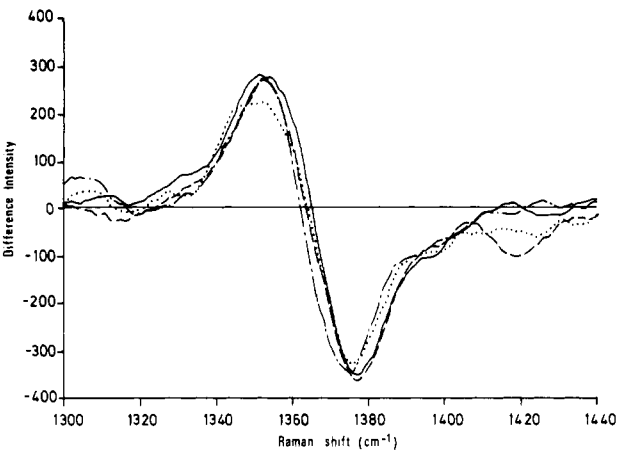

FIGURE 4: Resonance Raman difference spectra obtained by subtracting the equilibrium HbCO spectrum from various HbCO photoproduct spectra: 9.4 (···), 30 (– – –), 95 ps (–·–), and equilibrium unligated Hb (—). The increase in the downshift of these spectra with respect to that of equilibrium unligated Hb as a function of time is interpreted in terms of a developing interaction between the proximal histidine and the porphyrin. This interaction is attributed to relaxation of the protein.

(3) Both a shift and a broadening of the photoproduct can change the position of the inflection point. Specifically, the effect of broadening in the photoproduct is to diminish its apparent shift.

The shift of the ν_4 band in the HbCO photoproduct with respect to its value in unligated equilibrium Hb, $\Delta\nu_4$, is related to the position of the inflection point by

$$\Delta\nu_4 = 2\nu_{IP} - \nu_4(\text{HbCO}) - \nu_4(\text{Hb}) \qquad (1)$$

ν_{IP} is the frequency of the inflection point. ν_4(HbCO) and ν_4(Hb) are the center frequencies of the ν_4 band in the equilibrium spectra of HbCO and Hb, respectively. This calculation is only valid for spectral bands of identical intensity and shape. For such bands, the inflection point is simply the average value of the positions of the two maxima. This is a good approximation for the ν_4 bands of equilibrium HbCO and Hb, as can be seen from their nearly symmetric difference spectrum in Figure 2. This procedure was used to calculate the position of the ν_4 bands of the HbCO photoproducts at times greater than or equal to 9.4 ps subsequent to photodissociation (Table I).

The spectral broadening of the HbCO photoproduct at times up to at least 2 ps yields asymmetric difference spectra. In this case eq (1) cannot be used directly to calculate the spectral shift because the broadening of the photoproduct gives an underestimate of the shift. To determine the broadening in the spectra of the HbCO photoproducts, we constructed the photoproduct spectra. This was done by subtracting an amount of the equilibrium spectrum (corresponding to 40 ± 5% photodissociation) from the time-resolved spectra. The reconstructed photoproduct spectra are fit to a Gaussian and deconvoluted from the instrument function of our Raman spectrometer. The Rayleigh of the 435-nm probe beam in HbCO is used as the instrument function. The Rayleigh is fairly well approximated by a Gaussian with 30-cm^{-1} fwhm; i.e., it represents only the spectrum of our transform-limited probe pulse. We use a value of 14.7 cm^{-1} for the fwhm of ν_4 in equilibrium unligated Hb (Friedman et al., 1982a,b) to calculate the spectra broadening in the photoproduct. The spectral shift is then estimated by subtraction of the value of the broadening from eq 1. These data are summarized in Table I. We are confident in the values of the shift of the HbCO photoproduct to within ±2 cm^{-1}.

Table I: Summary of Data from Time-Resolved Raman Spectra

time (ps)	ν_{IP}[a] (cm^{-1})	ν_4 of HbCO photoproduct[b] (cm^{-1})	$\Delta\nu_4$[c] (cm^{-1})	increase in heme temp[d] (K)
0.9	1360.4	1347.8	−9.0 (−11.0)	218
2	1361.6	1350.2	−6.6 (−7.6)	149
9.4	1363.8	1354.6	−2.2	45
30	1363.4	1353.8	−3.0	
95	1361.8	1350.6	−6.2	
equil Hb	1364.9	1356.8[e]	0	

[a] The position of the inflection point of the difference spectrum created by subtraction of the equilibrium HbCO spectrum from the HbCO photoproduct spectrum. See Figures 3 and 4. [b] The calculated position of the ν_4 band of the photoproduct—assuming it is not spectrally broadened—from the ν_4 band of the equilibrium unligated Hb. See text and eq 1. [c] The spectral shift of the ν_4 band of the HbCO photoproduct with respect to the ν_4 of the equilibrium unligated Hb. The values in parentheses for the 0.9- and 2-ps spectra are corrections made for the spectral broadening of the photoproducts with respect to the equilibrium unligated Hb. The estimated confidence in these values is ±2 cm^{-1}. [d] The temperature difference of the heme in the HbCO photoproduct with respect to that of the equilibrium unligated Hb at 288 K. The temperature was calculated from eq 4. The estimated error in the temperature determination is ±48 K. For times subsequent to 9.4 ps, heme temperatures are not calculated because the observed increase in ν_4 is attributed to protein relaxation. Because of the presence of Hb^*_I, the 0.2-ps spectrum is sufficiently complicated that a temperature is not estimated. See text. [e] This value represents the position of the ν_4 band of the equilibrium unligated Hb as calculated from its difference spectrum with HbCO (Figure 2a) as described in the text. The calculated value agrees with that obtained from the spectrum in Figure 1a (1357 cm^{-1}) to within the frequency separation of adjacent pixels of our detector (0.8 cm^{-1}).

RESULTS

(A) Equilibrium Spectra of Hb and HbCO. Figure 2 presents the equilibrium resonance Raman spectra of Hb and of HbCO measured with the probe beam only and their difference spectrum. In the HbCO spectrum, several bands in the region from 1200 to 1650 cm^{-1} were observed whose assignments have been based on the results of spectra from model compounds and from normal mode calculations (Kitagawa et al., 1978; Abe et al., 1978; Spiro & Burke, 1976; Choi et al., 1982): (1) 1236 cm^{-1}, ν_{13} C_mH bend; (2) 1373 cm^{-1}, ν_4 $C_\alpha N$ stretch; (3) 1494 cm^{-1}, ν_3 $C_\alpha C_m$ stretch; (4) congestion in the high-frequency region of the spectrum (1550–1660 cm^{-1}). This region contains contributions from the Soret-enhanced modes ν_{38} $C_\alpha C_m$ stretch, ν_2 $C_\beta C_\beta$ stretch, ν_{37} $C_\beta C_\beta$ stretch, and from a vinyl carbon–carbon double-bond stretch (Dasgupta & Spiro, 1986). There are small contributions as well from modes that are enhanced with Q-band (550–580 nm) excitation. These bands are ν_{11} $C_\beta C_\beta$ stretch, ν_{19} $C_\alpha C_m$ stretch, and ν_{10} $C_\alpha C_m$ stretch (Dasgupta & Spiro, 1986).

The salient characteristics of the Hb–HbCO difference spectrum are the following: (1) the apparent absence of the ν_{13} and ν_3 bands; (2) the downshift and diminution of the congested high-frequency (1550–1650 cm^{-1}) region of the spectrum; (3) the shift of the ν_4 band to 1357 cm^{-1}, the value characteristic of unligated equilibrium Hb. The band at 1357 cm^{-1} has approximately the same shape and amplitude as its counterpart at 1373 cm^{-1}. This is easily discerned from the symmetry of the equilibrium Hb–HbCO difference spectrum.

(B) Time-Resolved Spectra of the HbCO Photoproducts. Our measurements are most sensitive to changes in the ν_4 band. At 0.2 ps, the band at 1373 cm^{-1} characteristic of ligated ferrous hemes has completely disappeared. The most striking features of the difference spectra are the asymmetries of the 0.2- (Figure 2), 0.9-, and 2-ps spectra (Figures 3 and 4): the band in the 1357-cm^{-1} region has not achieved the maximum amplitude of that of the equilibrium unligated Hb. Furthermore, there is a considerable downshift of ~5 cm^{-1} of the difference spectrum of the 0.9-ps photoproduct with respect to that of the equilibrium difference spectrum. All the photoproduct spectra are downshifted from the equilibrium spectrum (Table I, Figures 3 and 4). This shift decays to a minimum at approximately 10 ps and then begins to increase, attaining a value of 6.2 ± 2 cm^{-1} at 95 ps.

DISCUSSION

(I) Heme Photophysics

(A) Early-Time Temporal Evolution of the ν_4 Mode of the HbCO Photoproduct. The most notable features of the difference spectra of the HbCO photoproducts are the asymmetries of the early-time difference spectra and their shifts from the equilibrium difference spectrum. An attractive explanation for these phenomena is that a photon energy in excess of the Fe–CO bond energy heats the heme and produces spectral changes in the high-frequency modes via anharmonic coupling with thermally populated low-frequency modes of the heme (Dasgupta et al., 1985; Asher & Murtaugh, 1983). Performing a study of the temperature dependence of the Raman spectra of Ni(II) octaethylporphine (NiOEP) between 40 and 600 K, Asher and Murtaugh (1983) observed frequency downshifts as large as 15 cm^{-1} for the ν_{11}, ν_{19}, and ν_{10} modes (those modes especially sensitive to the core size of the heme). Assuming a specific heat of 0.5 cal/(K·g) for the heme, they concluded that temperature increases of ~90 K are expected to occur upon photolysis of HbCO or MbCO with 576-nm excitation (50 kcal/mol). They concluded that a transient Raman spectrum of sufficient time resolution would detect temperature-induced downshifts of these modes of ~5 cm^{-1}.

Several experiments have been performed that give an indication of the time scale required for vibrational cooling in optically excited molecules. Hochstrasser and co-workers (Greene et al., 1979; Doany et al., 1980) have shown that the transient absorption spectrum of *trans*-stilbene in hexane changed shape during the first 50 ps following excitation with 265-nm laser pulses (6450 cm^{-1} of excess energy). And Seilmeier et al. (1984) detected an increase in the absorption of the long-wavelength tail of the dye oxazine 1 in ethanol when the CH_3 groups of the dye were directly excited. This absorption change was found to decay with a time constant of 10 ps. Finally, using molecular dynamics simulations, Henry et al. (1986a,b) have determined that in unligated Mb, without Fe or hydrogen atoms and in vacuo, at room temperature the complete conversion of a 530-nm photon (54 kcal/mol) into vibrational energy initially raises the temperature of the heme by 500 K. The cooling of the heme is suggested to occur by means of van der Waals or near-neighbor contacts between the protein and the heme. It is estimated that there are 100 such contacts within 5 Å of the heme. The decay of the vibrational temperature was determined to be nonexponential with 50% cooling occurring in 1–4 ps and the remainder in 20–40 ps.

The temperature-dependent Raman spectra of Asher and Murtaugh and the time scale for vibrational cooling determined by both experiments and in computer simulations have prompted us to consider the effect of a vibrationally hot heme on our time-resolved Raman spectra.

(B) Influence of Vibrationally Hot Hemes on the Time-Resolved Raman Spectrum. A model for vibrational dephasing by inter- or intramolecular vibrational energy exchange has been developed by Harris and co-workers (Harris et al., 1977, 1978; Shelby et al., 1979; Marks et al., 1980) and

has been used by Asher and Murtaugh (1983) to interpret their Raman spectra. In this model, dephasing of a given high-frequency mode results from random modulation due to energy exchange with a specific low-frequency mode. The important features of the model are the following. When a high-frequency mode interacts with a low-frequency mode, the high-frequency mode will shift to a value, ν, where

$$\nu = \nu^0 + \frac{e^{-E_i/kT}\delta\nu}{[1 + (\delta\nu)^2\tau^2]} \quad (2)$$

and where ν^0 is the position of the band in the low-temperature limit. The width of the new band will be broadened to $(T_2)^{-1}$, where

$$(T_2)^{-1} = (T_2^0)^{-1} + \frac{e^{-E_i/kT}(\delta\nu)^2\tau}{[1 + (\delta\nu)^2\tau^2]} \quad (3)$$

and where $(T_2^0)^{-1}$ is the width of the band in the low-temperature limit. The quantity $\delta\nu$ gives the strength of the interaction produced by the anharmonic coupling. $\delta\nu$ can be either positive or negative depending on the nature of the coupling between modes. τ represents the lifetime of the low-frequency mode to which the high-frequency mode is coupled. The frequency of this mode is given by E_i, the apparent "activation energy" in eq 2 and 3. An interesting consequence of this model is that both the shift and the broadening of the high-frequency mode have the same temperature dependence.

Assuming that the model of Harris and co-workers can be applied to HbCO, we use eq 2, the values obtained from the analysis of the temperature dependence of the ν_{10} mode of NiOEP (Asher & Murtaugh, 1983), and our values for the spectral shift of the HbCO photoproduct to estimate the temperature increase in the HbCO photoproduct relative to that of the unligated equilibrium Hb as a function of time. The temperature difference as a function of time is given by

$$\Delta T(t) = \frac{-E_i/k}{\ln\left[\frac{\Delta\nu(t)}{M} + \exp(-E_i/kT_{Hb})\right]} - T_{Hb} \quad (4)$$

E_i is the activation energy obtained from the Arrhenius plot of the frequency shift of the ν_{10} mode vs $1/T$ and corresponds to the low-frequency mode to which the high-frequency mode is anharmonically coupled [528 ± 150 cm^{-1} (Asher & Murtaugh, 1983)]. $\Delta\nu(t) = \nu(t) - \nu_{Hb}$, where $\nu(t)$ is the frequency of ν_4 in the HbCO photoproduct and ν_{Hb} is the frequency of the ν_4 mode of the unligated equilibrium Hb (1357 cm^{-1}). M is the factor $\delta\nu/[1 + (\delta\nu)^2\tau^2]$ that appears in eq 2 and is equal to −73 cm^{-1}. T_{Hb} is the temperature of the unligated equilibrium Hb, which in our case is 288 K. At 0.9 ps, we estimate that the temperature of the heme is increased by 218 K from that of the unligated equilibrium heme (Table I).

This is in good agreement with the estimation of Asher and Murtaugh (1983). Our result that the heme has undergone significant vibrational cooling by 10 ps is in excellent agreement with the time scales of vibrational cooling measured in polyatomic molecules and with the results of molecular dynamics calculations. Our confidence (±2 cm^{-1}) in the position of the ν_4 bands of the photoproduct makes it difficult to determine whether the heme has completely cooled by 10 ps (Table I) or undergoes a slower cooling phase as indicated by the molecular dynamics simulations (Henry et al., 1986a,b). In order for us to compare properly our data with the simulations of Henry et al., it is necessary to note that in their calculation the *entire* energy of the 530-nm photon (54 kcal/mol) is used to heat the heme. Scaling the cooling curve of Henry et al. to take into account the Fe–CO dissociation energy [25 kcal/mol (Asher & Murtaugh, 1983; Keyes et al., 1971)], one obtains a temperature increase of ~140 K for the heme at 0.9 ps, which is in good agreement with our result.

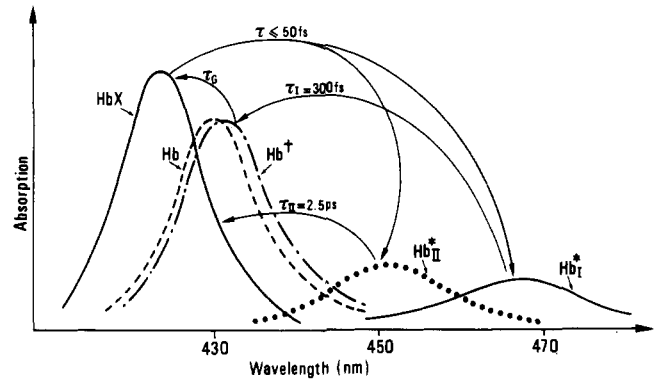

FIGURE 5: Generalized absorption spectra of heme proteins and their photoproducts. The interrelationships among these species are illustrated in the figure and described in more detail in the text and elsewhere (Martin et al., 1983, 1984a,b, unpublished data). X denotes the ligand—O_2, CO, or NO. The excited-state unligated species, Hb^*_I and Hb^*_{II}, are formed in less than 50 fs from the photoexcited HbX, but the amounts of Hb^*_I and Hb^*_{II} formed are dependent on X. τ_I is the time constant for the formation of the deoxy-like species from Hb^*_I. τ_{II} is the time constant for the decay of Hb^*_{II} to the ground-state species. τ_G is the time constant for geminate recombination and depends on the ligand, the heme protein, and allosteric effectors. The diagram is labeled for the case of hemoglobin, but it is equally applicable for myoglobin and protoheme—providing that the associated shapes and positions of the deoxy-like species denoted by the dagger (†) are taken into account (Martin et al., 1984a,b, unpublished data).

One might be tempted to attribute the incompletely developed band in the 1357-cm^{-1} region (Figure 3) to the presence of a transient heme photoproduct whose Raman spectrum is not enhanced with 435-nm excitation. Transient absorption spectroscopy has indeed identified such an excited-state species, Hb^*_I, that absorbs from 470 to 500 nm. This species has been shown to decay in 300–350 fs to a deoxy-like product (Martin et al., 1983, 1984a; Petrich et al., 1987) (Figure 5), and thus at 0.9 ps Hb^*_I cannot contribute more than 8% to the distortion of the observed Raman difference spectrum. (The presence of Hb^*_I contributes significantly, however, to the 0.2-ps spectrum). It is conceivable that this first phase in the relaxation of ν_4 includes contributions from transient interactions of the π electron system of the porphyrin ring with the distal side of the heme pocket, with the CO, or with the proximal histidine.

(II) Structural Responses of Hemoglobin to Deligation

(A) Response of the Heme: Formation of the Deoxy-like Product. Transient absorption measurements have shown that photodissociation of the ligand (O_2, CO, or NO) from the heme of Hb, Mb, or protoheme occurs in less than 50 fs (Martin et al., 1983, 1984a; Petrich et al., 1987). Our time-resolved Raman spectra are in accord with this observation: at 0.2 ps subsequent to photodissociation, the ν_4 band at 1373 cm^{-1} characteristic of ligated ferrous hemes has completely disappeared (Figure 2). Produced on the time scale of ligand detachment is the excited state, Hb^*_I, which decays in 300–350 fs to a deoxy-like species $Hb^\dagger$. The details of the heme photophysics are summarized schematically in Figure 5. $Hb^\dagger$ has an absorption spectrum resembling that of the equilibrium unligated heme except that it is distorted (Martin et al., 1983, 1984a, unpublished results; Petrich et al., 1987). This distortion persists for the maximum delay time permitted in the absorption measurement, 400 ps. The 300–350-fs time

constant may be interpreted as the time required for the transition from a planar heme with low-spin Fe ($S = 0$) to that of a partially or fully domed heme with high-spin Fe ($S = 2$). The persistence and the magnitude of the red shift may be interpreted in terms of the response of the protein matrix to the domed heme. The results, however, of neither transient absorption nor resonance Raman spectroscopies contain enough information to determine whether the Fe ($S = 0$) to Fe ($S = 2$) spin transition occurs upon ligand photodissociation or accompanies the appearance of the deoxy-like product.

The role of the spin transition on the doming of the heme is uncertain. For example, calculations (Rohmer et al., 1983; Olafson et al., 1977) suggest that the out-of-plane displacement of the Fe is not due to the larger size of the high-spin Fe (Perutz, 1979) but rather to nonbonded interactions between the proximal histidine and the pyrrole nitrogens of the heme. Consistent with this interpretation is that removal of the sixth ligand, without change of the Fe spin state, is sufficient to produce at least half of the full doming of the heme (Perutz et al., 1979; Scheidt & Piciulo, 1976; Scheidt & Frisse, 1975).

The results of EXAFS measurements of photodissociated MbCO at 4 K (Chance et al., 1980) indicate that the CO is displaced by only 0.05 Å from the Fe and that the Fe–proximal histidine bond is lengthened by only 0.02 Å. A considerable body of data strongly suggests, however, that at room temperature displacements of the CO and of the proximal histidine are rapid and that they are greater than 0.05 Å and 0.02 Å, respectively. For example, molecular dynamics calculations (Henry et al., 1985) have shown that upon simulating dissociation of CO from Mb the Fe moves out of the heme plane in 50–150 fs. The observation of the ν_{Fe-His} mode in both the HbCO and MbCO photoproducts at 25 ps (Findsen et al., 1985a,b) is strong evidence (Kitagawa et al., 1979) for a rapidly domed heme. And the bleaching of the Soret band in less than 50 fs and the disappearance of the ν_4 band at 1373 cm^{-1} in less than 0.2 ps (Figure 2) suggest that very soon after photodissociation the CO is no longer sensed by the heme.

(*B*) *Implications for Hemoglobin Reactivity*. Two experiments have recently been performed that isolate a portion of the strain energy in Hb and that suggest a time scale for its transmission to the intersubunit contacts.

First, Findsen et al. (1985a) have studied the stretching frequency between the heme Fe and the proximal histidine, ν_{Fe-His}, in (carbonmonoxy)hemoglobins that, due to either allosteric effectors or genetic factors, possessed an R or T *ligated* equilibrium structure. The ν_{Fe-His} mode is an ideal marker of the interactions of the heme with the surrounding protein because it is present only in the Raman spectra of five-coordinate hemes. Its presence is taken to be the criterion of a domed, high-spin, heme (Kitagawa et al., 1979). These authors observed that 25 ps subsequent to photolysis the value of ν_{Fe-His} was already fully developed. Furthermore, the value of ν_{Fe-His} was dependent on the quaternary state of the hemoglobin before dissociation: at 25 ps, as at 10 ns, the greater the initial amount of ligated T conformation of the hemoglobin, the lower the value of ν_{Fe-His}. Because large-scale tertiary and quaternary structure changes in hemoglobin are thought to occur on time scales longer than 25 ps (Hofrichter et al., 1983), they reasoned that 25 ps was not enough time to delocalize the strain energy induced by ligand dissociation and that the strain energy had appeared in the value of ν_{Fe-His}, which correlated well with the quaternary structure of the undissociated hemoglobin. These results were incorporated into a detailed model for hemoglobin cooperativity in which the tilt angle of the proximal histidine with respect to the heme plane plays a crucial role, as proposed earlier by Gelin and Karplus (1977). Specifically, the strain energy responsible for a high value of ν_{Fe-His} is reduced by a tilt of the proximal histidine with respect to the heme plane. They suggest that earlier investigations (Rousseau et al., 1984; Rousseau & Ondrias, 1985; Nagai et al., 1980; Tsubaki et al., 1982; Tsubaki & Yu, 1980) failed to discover a localization of strain energy because they focused on the R and T structures of the ligated proteins *at equilibrium*. Most importantly, Findsen et al. provide an upper limit of 25 ps for the time scale required for investigating the manifestation of the strain energy induced by ligand dissociation.

Second, Dasgupta et al. (1986) have used 7-ns pulses at 218 nm to study the changes in the resonance Raman spectra of the tryptophyl and tyrosyl residues in the $\alpha_1\beta_2$ interface of photodissociated HbCO and HbO_2. Their results suggest that in less than 7 ns the $\alpha_1\beta_2$ interface is in a "T-like" configuration.

Our resonance Raman spectra taken at times from 0.9 to 95 ps can be interpreted in terms of two transient responses of the heme in the HbCO photoproduct (Table I). The first has been suggested to be rapid vibrational cooling that is substantially complete by 10 ps. Second, the downshift of ν_4 in the HbCO photoproduct with respect to that of the equilibrium unligated heme slowly begins to increase after 10 ps. We interpret the increase of the ν_4 downshift in terms of the results of transient absorption (Martin et al., 1983, 1984a; Petrich et al., 1987) and resonance Raman experiments (Findsen et al., 1985a; Dasgupta et al., 1986). A partly or fully domed deoxy-like heme is produced with a time constant of 350 fs in HbCO. A tight coupling of the heme Fe through the proximal histidine and the F-helix produces a T-like change at the $\alpha_1\beta_2$ contacts in approximately 30 ps. This T-like change is effected by a translation of the F-helix across the heme plane (Gelin & Karplus, 1977; Baldwin & Chothia, 1979). The motion of the F-helix produces a tilt [and, perhaps, a rotation (Phillips, 1980; Shaanan, 1983)] of the proximal histidine with respect to the heme plane. The tilting increases the interaction of the proximal histidine with the π electron system of the porphyrin ring. This results in an increase of the electron density in the π^* antibonding orbitals of the porphyrin ring, which weakens the $C_\alpha N$ bond and hence downshifts the ν_4 band. At 95 ps subsequent to photodissociation, the value of the ν_4 downshift is 6.2 ± 2 cm^{-1} (Table I). This value is greater than that obtained at 10 ns for the HbCO photoproduct, 2.5 cm^{-1} (Friedman et al., 1982a,b). It is possible that the difference between these two values reflects another slow relaxation phase of the protein.

(*C*) *Correlation between ν_{Fe-His} and ν_4*. The downshifted value of ν_4 in the HbCO photoproducts with respect to its value in equilibrium unligated Hb has been well correlated with the value of ν_{Fe-His} in normal, mutant, and hybrid hemoglobins with various ligands and in the presence and absence of allosteric effectors in a study using 10-ns photodissociation pulses (Friedman et al., 1982a; Ondrias et al., 1982). In a pump–probe resonance Raman experiment with 30-ps pulses, Campbell and Friedman (1986) have shown that at 120 ps neither the position nor the shape of the ν_{Fe-His} band has changed from their values at zero time. Their spectra of the ν_4 mode, however, seem to indicate a downshift evolving from the value at zero time to 140 ps subsequent to photodissociation. If so, this is consistent with our above suggestion that the major factor contributing to the correlation between ν_{Fe-His} and ν_4, the tilting of the proximal histidine, is not established until approximately 30 ps subsequent to photodissociation. The

long-lasting correlation between ν_{Fe-His} and ν_4 can be explained by a structural response of the protein accompanied by the T-like change at the $\alpha_1\beta_2$ interface (Dasgupta et al., 1986). The tetrameric structure of hemoglobin is associated with a variety of slowly relaxing shifts in resonance Raman and transient absorption spectroscopies, notably: (1a) the downshift of ν_4 in the HbCO photoproduct with respect to its value in equilibrium unligated Hb persists from 10 ns to 1 ms (Friedman & Lyons, 1980; Lyons & Friedman, 1982). At 10 ns, ν_4 in the HbCO photoproduct was downshifted by a little less than 2 cm^{-1} from its value in equilibrium unligated Hb of 1357 cm^{-1}; and at 1 ms, ν_4 had not yet attained its equilibrium value. (1b) At 10 ns, no downshift of ν_4 is observed between the MbCO photoproduct and the equilibrium unligated Mb (Friedman et al., 1982a,b). (2a) The value of ν_{Fe-His} obtained at 25 ps for the HbCO photoproduct is 230 cm^{-1} and relaxes to $\sim$222 cm^{-1} in the equilbrium unligated species (Findsen et al., 1985a). (2b) The value of ν_{Fe-His} obtained at 25 ps for the MbCO photoproduct is the same as that of the equilibrium unligated Mb, $\sim$222 cm^{-1} (Findsen et al., 1985b). (3a) The transient absorption difference spectrum of the HbCO photoproduct is distorted from that of equilibrium unligated Hb (Martin et al., 1983, 1984a,b). The distortion of the photoproduct spectrum appears with a time constant of 300–350 fs. The spectrum attains the form of that of the equilibrium species in a series of slow processes characterized by 50-ns, 1-μs, and 20-μs time constants (Hofrichter et al., 1983). (3b) The transient absorption difference spectrum of the MbCO photoproduct is symmetric with a red shift of $\leq$1 nm from that of the equilibrium ligated Mb (Martin et al., unpublished data); and the absorption spectrum of the protoheme photoproduct is superimposable on the equilibrium spectrum (Martin et al., 1984a).

From these observations we can infer that the tetrameric structure of hemoglobin imposes a strained environment upon the heme–proximal histidine unit, which because of ligand dissociation is rapidly doming. The negligible red shift and the symmetry of the transient absorption difference spectrum of the MbCO photoproduct suggest that doming of the heme in Mb is not impeded by any significant resistance from the protein. Hence, in the MbCO photoproduct, ν_{Fe-His}, ν_4, and the transient absorption spectrum all rapidly attain their equilibrium values. We suggest that the tilting of the proximal histidine in the unrelaxed protein environment imposed by the tetrameric nature of Hb is the origin of the correlation between ν_{Fe-His} and ν_4.

On the basis of the data of Table I, it is reasonable to estimate that this correlation is present 30 ps subsequent to photodissociation. Our proposal that 30 ps is required to tilt the proximal histidine with respect to the already domed heme and to establish a concomitant T-like change at the $\alpha_1\beta_2$ interface is consistent with the results of Findsen et al. (1985a), indicating that the strain energy of cooperativity is initially located in the Fe–proximal histidine bond which is tightly coupled through the F-helix to the $\alpha_1\beta_2$ interface. Thus, the appearance of a change in another part of the protein with a fast but finite time constant is indicative of the flow of initially localized strain energy through a well-defined conduit.

(*D*) *Comparison of Time-Resolved Raman and Absorption Spectroscopies.* For the two relaxation phases observed in the downshift of the ν_4 mode of the HbCO photoproduct with respect to its value in equilibrium unligated Hb, corresponding relaxation phases are not detected in transient absorption spectroscopy obtained with the current levels of accuracy provided by subnanosecond spectrometers. Thus, the vibrational spectroscopy of the ν_4 mode has shown itself to be a more sensitive indicator of the changes in the heme and its environment than has electronic absorption spectroscopy. This is not particularly surprising, especially for the case of the Soret band that we have considered here. For example, Schomaker et al. (1984) present absorption spectra of cytochrome *c* at 110 and 298 K, where the maximum shifts from 413 nm to only 415 nm. Furthermore, the fwhm of the spectrum broadens by less than 10%. Similar results are observed in photosynthetic pigments (Hayworth et al., 1982). On the other hand, the Raman shift we estimate for the HbCO photoproduct at 0.9 ps (11 cm^{-1}) represents 75% of the fwhm of the band of the equilibrium unligated Hb (14.7 cm^{-1}).

If our assignment of the rapid relaxation of the ν_4 downshift is correct, then we may infer that the distortion of the transient absorption difference spectra of the HbCO photoproduct with respect to its equilibrium unligated counterpart is not an artifact due to vibrationally hot hemes, but a real protein-induced change of the electronic spectrum of the heme. This conclusion is further supported by the absence of any corresponding distortion in the transient absorption spectra of protoheme.

That vibrational cooling seems to be complete by 10 ps in the HbCO photoproduct suggests that the 200-ps absorption recovery phase of photodissociated HbO_2 is indeed geminate recombination of O_2 (Cornelius et al., 1981; Friedman et al., 1985). We cannot, however, be so sure of the assignment of the corresponding 13-ps absorption recovery of photodissociated HbNO (Houde et al., 1986; Cornelius et al., 1983). That is, while the effects of vibrational heating are not directly evident in the electronic absorption spectra of hemeproteins, this does not imply that vibrational heating is not present or that it does not influence the chemistry of ligand binding. Thus, the early stages of geminate recombination in HbNO should still be interpreted with caution.

Conclusions

We have developed a resonance Raman spectrometer capable of subpicosecond resolution. This tool will enable us to study the transient changes induced upon photodissociation of heme proteins with various ligands and in the presence of allosteric effectors in the time regime where the strain energy of cooperativity becomes localized. We have obtained spectra of the HbCO photoproduct at times from 0.2 to 95 ps. These studies concentrated on the high-frequency region of the Raman spectrum, especially on the shift and the broadening of the band corresponding to the $C_\alpha N$ stretching frequency (ν_4). Two trends are observed in the time evolution of ν_4.

First, the changes in its transient spectra are interpreted in terms of vibrational heating of the heme. An increase in the heme vibrational temperature of 218 K is determined at 0.9 ps subsequent to photodissociation. This value is in good agreement with the estimate of Asher and Murtaugh (1983) (90 K) and the simulations of Henry et al. (1986a,b) (140 K). Our results that the heme in the HbCO photoproduct has substantially cooled by 10 ps is in excellent agreement with both the time scales of vibrational cooling observed in large polyatomic molecules (Greene et al., 1979; Doany et al., 1980; Seilmeier et al., 1984) and with the molecular dynamics simulations of Henry et al., who determined that the vibrational temperature of photoexcited Mb decays to $\sim$50% of its initial value in 1–4 ps and that the remainder of the decay occurs in 20–40 ps. The agreement with molecular dynamics simulations is particularly encouraging because it fosters additional confidence in the use of such calculations as a tool for predicting the structure and dynamics of large molecules. The observation of vibrational cooling in HbCO suggests the

possibility of using the heme as a probe of the temperature changes of the heme pocket. For example, the effect of mutations of certain amino acids comprising the heme pocket might significantly alter the rate of vibrational cooling. Such data could yield information on the influence of different areas of the heme pocket on hemoglobin function. Second, the concomitant increase of the downshift of the ν_4 mode that can be characterized by a time constant of approximately 30 ps is attributed to the transmission of strain energy stored in the Fe–proximal histidine bond to the $\alpha_1\beta_2$ contacts.

ACKNOWLEDGMENTS

We thank B. Bohn for preparation of the samples.

Registry No. HbA, 9034-51-9; (HbA)CO, 9072-24-6; heme, 14875-96-8.

REFERENCES

Abe, M., Kitagawa, T., & Kyogoku, Y. (1978) *J. Chem. Phys. 69*, 4526.

Asher, S. A. (1981) *Methods Enzymol. 76*, 371.

Asher, S. A., & Murtaugh, J. (1983) *J. Am. Chem. Soc. 105*, 7244.

Baldwin, J. M., & Chothia, C. (1979) *J. Mol. Biol. 129*, 175.

Campbell, B. F., & Friedman, J. M. (1986) in *Ultrafast Phenomena* (Fleming, G. R., & Siegman, A. E., Eds.) Vol. V, p 423, Springer, Berlin.

Chance, B., Fischetti, B., & Powers, L. (1983) *Biochemistry 22*, 3820.

Choi, S., Spiro, T. G., Langry, K. C., Smith, K. M., Budd, D. L., & La Mar, G. N. (1982) *J. Am. Chem. Soc. 104*, 4345.

Cornelius, P. A., Steele, W. A., Chernoff, D. A., & Hochstrasser, R. M. (1981) *Proc. Natl. Acad. Sci. U.S.A. 78*, 7526.

Cornelius, P. A., Hochstrasser, R. M., & Steele, W. A. (1983) *J. Mol. Biol. 163*, 119.

Dasgupta, S., & Spiro, T. G. (1986) *Biochemistry 25*, 5941.

Dasgupta, S., Spiro, T. G., Johnson, C. K., Dalickas, G. A., & Hochstrasser, R. M. (1985) *Biochemistry 24*, 5295.

Dasgupta, S., Copeland, R. A., & Spiro, T. G. (1986) *J. Biol. Chem. 261*, 10960.

Doany, F. E., Greene, B. I., & Hochstrasser, R. M. (1980) *Chem. Phys. Lett. 75*, 206.

Findsen, E. W., Friedman, J. M., Ondrias, M. R., & Simon, S. R. (1985a) *Science (Washington, D.C.) 229*, 661.

Findsen, E. W., Scott, T. W., Chance, M. R., Friedman, J. M., & Ondrias, M. R. (1985b) *J. Am. Chem. Soc. 107*, 3355.

Fork, R. L., Shank, C. V., Yen, R., & Hirlimann, C. (1983) *IEEE J. Quantum Electron. QE-19*, 500.

Friedman, J. M., & Lyons, K. B. (1980) *Nature (London) 284*, 570.

Friedman, J. M., Rousseau, D. L., & Ondrias, M. R. (1982a) *Annu. Rev. Phys. Chem. 33*, 471.

Friedman, J. M., Stepnoski, R. A., Stavola, M., Ondrias, M. R., & Cone, R. L. (1982b) *Biochemistry 21*, 2022.

Friedman, J. M., Scott, T. W., Fisanick, G. J., Simon, S. R., Findsen, E. W., Ondrias, M. R., & Macdonald, V. W. (1985) *Science (Washington, D.C.) 229*, 187.

Gelin, B. R., & Karplus, M. (1977) *Proc. Natl. Acad. Sci. U.S.A. 74*, 801.

Greene, B. I., Hochstrasser, R. M., & Weisman, R. B. (1979) *Chem. Phys. Lett. 62*, 427.

Harris, C. B., Shelby, R. M., & Cornelius, P. A. (1977) *Phys. Rev. Lett. 38*, 1415.

Harris, C. B., Shelby, R. M., & Cornelius, P. A. (1978) *Chem. Phys. Lett. 57*, 8.

Hayworth, P., Tapie, P., Arntzen, C. J., & Breton, J. (1982) *Biochim. Biophys. Acta 682*, 152.

Henry, E. R., Levitt, M., & Eaton, W. A. (1985) *Proc. Natl. Acad. Sci. U.S.A. 82*, 2034.

Henry, E. R., Eaton, W. A., & Hochstrasser, R. M. (1986a) in *Ultrafast Phenomena* (Fleming, G. R., & Siegman, A. E., Eds.) Vol. V, p 430, Springer, Berlin.

Henry, E. R., Eaton, W. A., & Hochstrasser, R. M. (1986b) *Proc. Natl. Acad. Sci. U.S.A. 83*, 8982.

Hofrichter, J., Sommer, J. H., Henry, E. R., & Eaton, W. A. (1983) *Proc. Natl. Acad. Sci. U.S.A. 80*, 2235.

Houde, D., Petrich, J. W., Rojas, O. L., Poyart, C., Antonetti, A., & Martin, J. L. (1986) in *Ultrafast Phenomena* (Fleming, G. R., & Siegman, A. E., Eds.) Vol. V, p 419, Springer, Berlin.

Keyes, M. H., Falley, M., & Lumry, R. J. (1971) *J. Am. Chem. Soc. 93*, 2035.

Kitagawa, T., Iizuka, T., Ikeda-Saito, M., & Kyogoku, Y. (1976) *J. Am. Chem. Soc. 98*, 5169.

Kitagawa, T., Abe, M., Kyogoku, Y., Ogoshi, H., Sugimoto, H., & Yoshida, Z. (1977) *Chem. Phys. Lett. 48*, 55.

Kitagawa, T., Abe, M., & Ogoshi, H. (1978) *J. Chem. Phys. 69*, 4516.

Kitagawa, T., Nagai, K., & Tsubaki, M. (1979) *FEBS Lett. 104*, 376.

Laane, J., & Keifer, W. (1980) *J. Chem. Phys. 72*, 5305.

Lyons, K. B., & Friedman, J. M. (1982) in *Hemoglobin and Oxygen Binding* (Ho, C., et al., Eds.) p 333, Elsevier, Amsterdam.

Marks, S., Cornelius, P. A., & Harris, C. B. (1980) *J. Chem. Phys. 73*, 3069.

Martin, J. L., Poyart, C., Migus, A., Lecarpentier, Y., Astier, R., & Chambaret, J. P. (1982) in *Picosecond Phenomena* (Eisenthal, K. B., et al., Eds.) Vol. III, p 294, Springer, Berlin.

Martin, J. L., Migus, A., Poyart, C., Lecarpentier, Y., Astier, R., & Antonetti, A. (1983) *Proc. Natl. Acad. Sci. U.S.A. 80*, 173.

Martin, J. L., Migus, A., Poyart, C., Lecarpentier, Y., Astier, R., & Antonetti, A. (1984a) in *Ultrafast Phenomena* (Auston, D. H., & Eisenthal, K. B., Eds.) Vol. IV, p 447, Springer, Berlin.

Martin, J. L., Migus, A., Poyart, C., Lecarpentier, Y., & Antonetti, A. (1984b) in *Hemoglobin* (Schnek, A. G., & Paul, C., Eds.) p 173, University of Brussels, Brussels.

Martin, J. L., Breton, J., Hoff, A. J., Migus, A., & Antonetti, A. (1986) *Proc. Natl. Acad. Sci. U.S.A. 83*, 957.

Myers, A. B., Mathies, R. A., Tannor, D. J., & Heller, E. J. (1982) *J. Chem. Phys. 77*, 3857.

Nagai, K., Kitagawa, T., & Moimoto, H. (1980) *J. Mol. Biol. 136*, 2271.

Olafson, B. D., & Goddard, W. A. (1977) *Proc. Natl. Acad. Sci. U.S.A. 74*, 1315.

Ondrias, M. R., Rousseau, D. L., Shelnutt, J. L., & Simon, S. R. (1982) *Biochemistry 21*, 3428.

Perutz, M. F. (1976) *Br. Med. Bull. 32*, 195.

Perutz, M. F. (1979) *Annu. Rev. Biochem. 48*, 327.

Petrich, J. W., Houde, D., Poyart, C., Orszag, A., & Martin, J. L. (1987) *Photobiochem. Photobiophys. Suppl.*, 77.

Phillips, S. E. V. (1980) *J. Mol. Biol. 142*, 531.

Rohmer, M.-M., Dedieu, A., & Veillard, A. (1983) *Chem. Phys. 77*, 449.

Rousseau, D. L. (1981) *J. Raman Spectrosc. 10*, 94.
Rousseau, D. L., & Ondrias, M. R. (1985) *Biophys. J. 47*, 726.
Rousseau, D. L., Tan, S. L., Ondrias, M. R., Ogawa, S., & Noble, R. W. (1984) *Biochemistry 23*, 2857.
Scheidt, W. R., & Frisse, M. E. (1975) *J. Am. Chem. Soc. 97*, 17.
Scheidt, W. R., & Piciulo, P. L. (1976) *J. Am. Chem. Soc. 98*, 1913.
Schomaker, K. T., & Champion, P. M. (1986) *J. Chem. Phys. 84*, 5314.
Schomaker, K. T., Bangcharoenpaurpong, O., & Champion, P. M. (1984) *J. Chem. Phys. 80*, 4701.
Seilmeier, A., Scherer, P. O. J., & Kaiser, W. (1984) *Chem. Phys. Lett. 105*, 140.
Shaanan, B. (1983) *J. Mol. Biol. 171*, 31.
Shelby, R. M., Harris, C. B., & Cornelius, P. A. (1979) *J. Chem. Phys. 70*, 34.
Spiro, T. G., & Burke, J. M. (1976) *J. Am. Chem. Soc. 98*, 5482.
Terner, J., Stong, J. D., Spiro, T. G., Nagumo, M., Nicol, M. F., & El-Sayed, M. A. (1981) *Proc. Natl. Acad. Sci. U.S.A. 78*, 1313.
Tsubaki, M., & Yu, N.-T. (1982) *Biochemistry 21*, 1140.
Tsubaki, M., Nagai, K., & Kitagawa, T. (1980) *Biochemistry 19*, 379.
Tsubaki, M., Srivastava, R. B., & Yu, N.-T. (1982) *Biochemistry 21*, 1132.
Yamamoto, T., Palmer, G., Gill, D., Salmeen, I. T., & Rimai, L. (1973) *J. Biol. Chem. 248*, 5211.

Electron–Nuclear Coupling in Nitrosyl Heme Proteins and in Nitrosyl Ferrous and Oxy Cobaltous Tetraphenylporphyrin Complexes†

Richard S. Magliozzo,* John McCracken, and Jack Peisach
Department of Molecular Pharmacology, Albert Einstein College of Medicine, Bronx, New York 10461
Received April 29, 1987; Revised Manuscript Received July 2, 1987

ABSTRACT: Electron spin echo envelope modulation (ESEEM) spectroscopy has been used to study electron–nuclear interactions in the following isoelectronic $S = {}^1/_2$ complexes: NO–Fe^{II}(TPP) (TPP = tetraphenylporphyrin) with and without axial nitrogenous base, nitrosylhemoglobin in R and T states, and O_2–Co^{II}(TPP) with and without axial base. Only the porphyrin pyrrole nitrogens contribute to the ESEEM of the 6-coordinate nitrosyl Fe^{II}(TPP) complexes, nitrosylhemoglobin (R-state), and the nitrosyl complexes of α and β chains. Pyrrole nitrogens in the 5-coordinate complex NO–Fe^{II}(TPP) are coupled too weakly to unpaired spin and therefore do not contribute to the ESEEM. A partially saturated T-state nitrosylhemoglobin does not exhibit echo envelope modulations characteristic of 6-coordinate nitrosyl species, which confirms that the proximal imidazole bond to heme iron is disrupted. Study of 6-coordinate O_2–Co^{II}(TPP)(L) complexes (L = nitrogenous base) using ^{14}N- and ^{15}N-labeled ligands and porphyrins enabled a detailed analysis of coupling parameters for both pyrrole and axial nitrogens. The pyrrole ^{14}N coupling frequencies are similar to those in NO–Fe^{II}(TPP)(L). The Fermi contact couplings for axially bound nitrogen, calculated from simulation of ESEEM spectra for a series of O_2–Co^{II}(TPP)(L) complexes (L = pyridine, 4-picoline, 4-cyanopyridine, 4-carboxypyridine, and 1-, 2-, and 4-methylimidazole) illustrate a trend toward stronger hyperfine interactions with weaker bases.

The magnetic resonance properties of metalloporphyrin complexes can often provide insight into the biochemistry of heme proteins. An understanding of the interactions between unpaired electron spin and nearby nuclei in metalloporphyrins enables the spectroscopist to address the effects on these interactions imposed by the protein in which the metalloporphyrin resides and to relate the prosthetic group properties to the tertiary and quaternary structure of that protein.

Electron paramagnetic resonance spectroscopy has been extensively used in studies of high- and low-spin ferric heme proteins (Blumberg et al., 1968; Peisach et al., 1971; Chevion et al., 1977; Hollenberg et al., 1980; Palmer, 1985) and ferrous nitrosyl heme proteins (Kon, 1968; Yonetani et al., 1972; Chevion et al., 1977; Hille et al., 1979; Morse & Chan, 1980; Hori et al., 1981; LoBrutto et al., 1983). These studies, in general, have addressed the identity of axial ligands to heme iron. An application of EPR[1] and ENDOR techniques to the chemistry of allosterism in hemoglobin has provided evidence for the disruption of the proximal imidazole Fe–N bond in the α subunits of nitrosylhemoglobin A in the low-affinity form, or T state (Höhn et al., 1983). The lability of this bond is suggested by a body of evidence for nitrosylhemoglobins (Szabo & Perutz, 1976; Nagai et al., 1980; Ascenzi et al., 1981).

Pulsed EPR techniques and the observation of electron spin echo modulations can also be used to study the biochemistry of hemoglobin. Electron spin echo envelope modulation spectroscopy, in its application to high- and low-spin d^5 heme proteins and iron metalloporphyrins, allows assignment of

† This work was supported by Grants HL-13399 and RR-02583 from the National Institutes of Health.

[1] Abbreviations: EPR, electron paramagnetic resonance; ENDOR, electron nuclear double resonance; ESEEM, electron spin echo envelope modulation; TPP, tetraphenylporphyrin; PPIX, protoporphyrin IX; imid, imidazole; pyr, pyridine; IHP, inositol hexaphosphate; Hb, hemoglobin; NQR, nuclear quadrupole resonance; nqi, nuclear quadrupole interaction; PAS, principal axis system; DEAE, dimethylaminoethyl; Tris, tris(hydroxymethyl)aminomethane.

0006-2960/87/0426-7923$01.50/0 © 1987 American Chemical Society